S.L.Lloyd
QMW London
7 February 2000
Updated 6 April 2000
ATL-V-EN-0001

Preliminary Investigation of Proposed Changes to the ATLAS Beam Pipe Geometry using FLUKA

This note presents preliminary results of an investigation into a number of proposed changes to the ATLAS beam pipe using the particle transport program FLUKA[1].

The ATLAS geometry as described in the ATLAS Technical Co-ordination Technical Design Report[2] has been implemented in FLUKA by Ian Dawson, using the geometrical description program ALICE[3]. This baseline implementation is referred to in this note as **AV5** (ATLAS Version 5). Figures 1 and 2 show the overall geometrical description as implemented in FLUKA while figures 3 to 6 show the VI, VA, VT and VJ sections of the beam pipe in more detail.

A number of changes have been implemented and the results compared to the baseline AV5 configuration. These are:

AV5_11 The Stainless Steel parts of the VI section of the beam pipe were changed to Aluminium with the thickness being increased by a factor of 1.5 to compensate. The inner diameter of the beam pipe and the outer diameter of the NEG section were kept fixed.

AV5_41 The Stainless Steel parts of the VI, VA, VT and VJ sections of the beam pipe were changed to Aluminium with the thickness being increased by a factor of 1.5 to compensate.

AV5_5 The Stainless Steel parts of the VI, VA, VT and VJ sections of the beam pipe were changed to Aluminium with the thickness being increased by a factor of 1.5 to compensate. The Aluminium parts of the VJ section of the beam pipe and flanges were changed to Stainless Steel and the thickness was decreased by a factor of 1.5 to compensate.

AV5_6 The VI section was replaced by two Beryllium pipes over the whole length $| z |<$ 363mm, each 0.8mm thick with the inner diameter of the inner pipe being 58mm and the outer diameter of the outer pipe being 70mm. The FLUKA geometry for this configuration is shown in figure 7. None of the other changes described above were implemented for this configuration.

AV5_7 The VI section was replaced by two Beryllium pipes over the length $| z |<$ 275mm, each 0.8mm thick and two Aluminium pipes over the length 275mm$<| z |<$ 363mm, each 1.1mm thick. The inner diameter of the inner pipes being 58mm and the outer diameter of the outer pipes being 70mm. None of the other changes described above were implemented for this configuration. Hence this configuration is the same as AV5_6 except that ends of the Beryllium pipes are replaced by slightly thicker Aluminium.

AV5_71 This configuration was the same as the previous AV5_7 except that the inner diameter of the pipes was reduced from 58mm to 54mm and the outer diameter of the pipes was reduced from 70mm to 66mm.

To summarise, the configurations were:

AV5_11 VI Stainless Steel changed to Aluminium.

AV5_41 VI, VA, VT and VJ Stainless Steel changed to Aluminium.

AV5_5 VI, VA, VT and VJ Stainless Steel changed to Aluminium. VJ Aluminium changed to Stainless Steel.

AV5_6 VI changed to 2 Beryllium pipes.

AV5_7 VI changed to 2 Beryllium plus Aluminium pipes.

AV5_71 Diameters of VI Beryllium and Aluminium pipes reduced by 4mm.

The results are presented in the tables on the following pages. The numbers represent the percentage change in fluence with respect to the baseline, AV5, at selected boundary crossings throughout ATLAS. The results are based on approximately 3,000 fully simulated (analogue) FLUKA p-p events at 14TeV for the baseline AV5 and approximately 1,500 such events for the other configurations. The results for neutrons and photons have reasonably high statistics everywhere, however the charged particle results are statistically limited, especially in the outer parts of the detector. Entries of zero usually mean that no particles were registered in that region for either FLUKA run and hence no conclusion can be drawn in that case.

Apart from the last configuration where the diameters was reduced, the percentage differences are rather small. The rates in the inner detector tend to go down when Stainless Steel is replaced by Aluminium and up when Aluminium is replaced by Stainless Steel or Beryllium by Aluminium as expected from the relative nuclear interaction lengths. The double Beryllium VI beam pipe is slightly better than the baseline whereas the Beryllium plus Aluminium ones are about the same.

Reducing the diameters of the pipes by 4mm clearly increases the rates by about 10%. This is what one would expect given that most particles from the p-p collisions go forward and hence are more likely to interact in the VI beam pipe if its diameter is reduced.

Hence the preliminary conclusion is that as long as the diameter is not reduced the proposed changes will have no detrimental effect on neutron and photon rates within ATLAS and are probably slightly beneficial in some cases. More statistics or the implementation of weighting in FLUKA are required to draw final conclusions about the rates of charged particles.

References

[1] FLUKA-98 Version 0.5, A.Fasso, A.Ferrari, P.Sala, J.Ranft, March 1999.

[2] ATLAS Technical Co-ordination Technical Design Report, CERN/LHCC/99-01, ATLAS TDR 13, January 1999.

[3] ALIFE: A Geometry Editor and Parser for FLUKA, A.Morsch.

Percentage change with respect to AV5

	AV5 11	AV5 41	AV5 5	AV5 6	AV5 7	AV5 71
1st Pixel Barrel						
n	-3.4 ± 3.9	-6.7 ± 3.7	4.1 ± 4.1	-1.0 ± 4.5	2.9 ± 4.1	8.8 ± 4.1
γ	22.3 ± 18.4	-2.3 ± 3.1	8.8 ± 6.0	5.5 ± 6.5	3.2 ± 3.3	5.5 ± 2.7
μ	-9.5 ± 6.4	-4.8 ± 6.2	3.2 ± 6.8	-13.5 ± 5.8	-10.3 ± 5.2	11.9 ± 6.5
$h^{\pm}$	-1.6 ± 2.9	-1.6 ± 3.1	3.1 ± 2.7	-1.6 ± 2.9	0.8 ± 2.5	7.0 ± 2.7
$e^{\pm}$	-12.3 ± 6.2	-5.2 ± 6.7	-9.7 ± 5.8	0.6 ± 6.3	2.6 ± 5.8	5.2 ± 5.9
$\pi^{\pm}$	-1.8 ± 2.9	-1.8 ± 3.1	2.7 ± 2.6	-1.8 ± 2.9	0.9 ± 2.4	7.3 ± 2.7
p	-6.3 ± 4.5	2.6 ± 4.3	4.7 ± 4.6	-0.2 ± 4.2	1.6 ± 4.0	9.2 ± 3.8
3rd Pixel Barrel						
n	-2.1 ± 3.4	-0.5 ± 3.5	4.2 ± 4.3	1.0 ± 3.6	0.8 ± 3.2	13.6 ± 6.6
γ	21.1 ± 19.8	-5.4 ± 6.9	3.9 ± 8.4	-6.4 ± 5.4	-4.4 ± 5.0	3.4 ± 5.2
μ	-0.9 ± 5.0	-4.3 ± 5.0	-0.9 ± 4.8	-7.8 ± 4.6	-8.7 ± 4.1	6.1 ± 5.6
$h^{\pm}$	-1.4 ± 3.0	-0.7 ± 3.2	3.9 ± 2.8	-1.1 ± 2.9	0.4 ± 2.5	8.4 ± 2.6
$e^{\pm}$	4.6 ± 8.6	-1.2 ± 6.1	-1.5 ± 6.2	-5.4 ± 7.0	0.1 ± 6.0	6.2 ± 5.6
$\pi^{\pm}$	-0.8 ± 3.0	-1.2 ± 3.2	3.7 ± 2.7	-0.8 ± 2.9	0.8 ± 2.5	8.1 ± 2.6
p	-5.8 ± 4.0	2.2 ± 4.4	5.8 ± 4.7	0.7 ± 4.2	-0.7 ± 4.3	10.2 ± 4.3
5th Pixel Disk						
n	-9.9 ± 3.5	-8.1 ± 3.7	-1.5 ± 4.0	-3.3 ± 4.0	-0.3 ± 4.3	5.9 ± 3.9
γ	-23.9 ± 16.4	-39.1 ± 14.5	-3.7 ± 26.4	-23.9 ± 19.3	-39.4 ± 14.6	-36.2 ± 14.4
μ	-8.6 ± 4.2	-3.1 ± 5.1	0.0 ± 5.0	-10.9 ± 4.5	-9.4 ± 4.6	3.9 ± 4.9
$h^{\pm}$	-4.0 ± 3.3	-3.3 ± 3.0	1.3 ± 2.9	-2.7 ± 3.2	2.0 ± 2.4	8.7 ± 3.0
$e^{\pm}$	-20.3 ± 13.4	-17.4 ± 13.2	-17.4 ± 13.3	-18.1 ± 13.4	-15.2 ± 13.2	-11.6 ± 13.3
$\pi^{\pm}$	-4.0 ± 3.2	-3.6 ± 3.0	1.6 ± 2.8	-2.8 ± 3.2	2.0 ± 2.5	8.4 ± 3.1
p	-6.1 ± 6.6	-3.7 ± 6.3	1.2 ± 6.5	-0.6 ± 7.1	0.0 ± 5.2	20.7 ± 5.7
1st SCT Barrel						
n	-5.0 ± 3.1	-2.9 ± 3.4	-0.9 ± 3.2	-1.5 ± 3.6	-2.9 ± 2.6	7.0 ± 3.1
γ	-35.0 ± 24.9	-48.8 ± 21.3	-45.3 ± 21.5	-37.6 ± 24.1	40.1 ± 79.8	-43.7 ± 21.3
μ	-1.5 ± 3.7	-2.3 ± 4.1	-0.7 ± 4.3	-5.8 ± 3.5	-0.5 ± 3.9	10.4 ± 4.6
$h^{\pm}$	-1.0 ± 3.1	-0.3 ± 3.2	3.1 ± 2.8	-0.4 ± 3.0	1.0 ± 2.6	10.2 ± 2.7
$e^{\pm}$	-0.9 ± 6.0	3.7 ± 6.4	1.7 ± 5.2	-1.4 ± 5.0	6.0 ± 6.5	16.0 ± 6.6
$\pi^{\pm}$	-1.0 ± 3.1	-0.9 ± 3.2	2.7 ± 2.8	-0.2 ± 3.0	1.2 ± 2.6	9.7 ± 2.7
p	-2.2 ± 3.7	2.6 ± 4.2	5.3 ± 3.8	0.7 ± 4.5	1.2 ± 4.1	14.6 ± 4.3
4th SCT Barrel						
n	-2.9 ± 3.2	-3.2 ± 3.2	0.0 ± 3.0	0.0 ± 3.4	-1.6 ± 2.7	8.3 ± 3.2
γ	-49.1 ± 19.4	-48.0 ± 19.4	-48.9 ± 19.4	-44.1 ± 19.9	-32.9 ± 23.5	-44.0 ± 19.9
μ	-3.6 ± 3.9	-4.4 ± 4.4	1.0 ± 4.4	-2.9 ± 4.0	0.7 ± 3.8	10.9 ± 5.1
$h^{\pm}$	-1.5 ± 3.1	-0.4 ± 3.6	3.9 ± 3.0	-0.8 ± 2.9	1.5 ± 2.6	10.0 ± 2.9
$e^{\pm}$	-4.1 ± 6.0	8.2 ± 7.5	0.0 ± 6.5	10.6 ± 7.4	3.5 ± 6.1	1.8 ± 6.6
$\pi^{\pm}$	-1.3 ± 3.0	0.0 ± 3.6	3.6 ± 3.0	0.0 ± 2.9	1.8 ± 2.6	9.9 ± 2.9
p	-5.9 ± 4.4	-2.7 ± 4.8	4.8 ± 4.5	-1.6 ± 4.9	0.5 ± 3.6	8.5 ± 4.3
9th SCT Disc						
n	-6.7 ± 3.5	-7.1 ± 3.0	-2.6 ± 3.1	-6.7 ± 3.1	-1.5 ± 2.8	6.4 ± 3.3
γ	-64.1 ± 18.7	-71.0 ± 18.3	-72.6 ± 18.2	-70.8 ± 18.5	-49.5 ± 26.3	-60.5 ± 20.1
μ	-0.5 ± 3.4	-2.5 ± 3.5	2.3 ± 3.3	-6.1 ± 3.9	-0.7 ± 2.9	10.0 ± 3.4
$h^{\pm}$	-4.4 ± 3.2	-4.0 ± 2.9	0.6 ± 2.9	2.0 ± 3.0	4.2 ± 2.5	11.8 ± 2.9
$e^{\pm}$	4.8 ± 10.8	0.9 ± 4.6	2.7 ± 4.4	7.8 ± 8.4	1.2 ± 3.5	12.0 ± 6.1
$\pi^{\pm}$	-4.6 ± 3.2	-3.6 ± 2.9	1.0 ± 2.9	1.2 ± 3.1	4.6 ± 2.5	11.3 ± 3.1
p	-4.6 ± 4.8	-9.2 ± 5.2	-5.7 ± 4.8	8.7 ± 5.2	3.5 ± 5.0	18.8 ± 4.2

Percentage change with respect to AV5

	AV5 11	AV5 41	AV5 5	AV5 6	AV5 7	AV5 71
Outer TRT Barrel						
n	-2.2 ± 3.3	-2.2 ± 3.6	1.7 ± 3.3	-1.7 ± 3.7	-1.7 ± 2.9	10.1 ± 3.2
γ	-41.3 ± 21.2	-44.7 ± 20.1	-45.9 ± 19.9	-33.5 ± 21.9	54.7 ± 96.4	-41.9 ± 20.0
μ	-8.2 ± 6.1	-5.8 ± 5.8	3.8 ± 7.3	-11.6 ± 6.0	-1.0 ± 5.6	8.2 ± 5.7
$h^{\pm}$	-3.7 ± 3.3	0.5 ± 3.9	3.7 ± 3.4	-2.3 ± 3.7	-2.1 ± 3.0	8.7 ± 3.2
$e^{\pm}$	2.8 ± 10.6	5.0 ± 17.6	-1.4 ± 11.1	-1.8 ± 12.3	7.8 ± 11.1	-7.3 ± 10.4
$\pi^{\pm}$	-2.9 ± 3.5	0.0 ± 4.0	2.3 ± 3.3	-2.1 ± 3.9	-3.5 ± 3.0	7.6 ± 3.4
p	-10.6 ± 4.7	-5.6 ± 5.2	7.8 ± 5.4	-5.0 ± 5.0	4.7 ± 4.8	8.4 ± 4.8
Outer TRT Wheel C						
n	-5.3 ± 3.7	-5.4 ± 3.8	-2.0 ± 2.9	-4.4 ± 3.4	-3.8 ± 2.8	3.8 ± 2.7
γ	-53.1 ± 36.6	-78.0 ± 29.6	-74.4 ± 29.6	-73.0 ± 30.0	-77.6 ± 29.6	-75.0 ± 29.6
μ	-10.8 ± 6.3	-8.4 ± 5.3	-3.1 ± 5.7	0.9 ± 7.1	-1.4 ± 5.8	5.0 ± 5.9
$h^{\pm}$	-16.8 ± 4.4	-12.1 ± 4.2	-14.3 ± 4.2	-16.0 ± 4.5	-10.3 ± 3.9	-2.0 ± 3.9
$e^{\pm}$	-14.4 ± 8.3	-8.3 ± 10.3	-13.5 ± 8.2	-20.0 ± 6.3	-14.9 ± 5.8	-12.0 ± 6.4
$\pi^{\pm}$	-11.5 ± 4.4	-8.6 ± 4.7	-11.2 ± 4.6	-8.6 ± 5.0	-5.0 ± 4.2	3.6 ± 4.9
p	-28.5 ± 6.5	-20.6 ± 6.1	-20.6 ± 6.4	-33.3 ± 6.2	-21.3 ± 6.2	-13.2 ± 6.0
Inner TRT Wheel C						
n	-6.6 ± 3.6	-9.4 ± 3.0	-6.7 ± 2.8	-8.9 ± 2.9	-5.2 ± 2.7	0.5 ± 2.8
γ	-58.3 ± 13.5	-74.8 ± 11.4	-68.5 ± 12.8	-65.9 ± 12.8	-54.2 ± 17.8	-69.6 ± 11.5
μ	-4.3 ± 4.2	-3.9 ± 4.1	-1.3 ± 4.2	-3.2 ± 4.0	-2.4 ± 3.3	10.8 ± 3.4
$h^{\pm}$	-16.7 ± 3.0	-15.8 ± 3.6	-10.4 ± 2.9	-23.9 ± 3.4	-11.7 ± 3.1	-6.8 ± 3.6
$e^{\pm}$	-82.5 ± 16.9	-84.5 ± 16.8	-83.1 ± 16.9	-82.8 ± 17.0	-81.4 ± 16.9	-79.4 ± 16.9
$\pi^{\pm}$	-12.3 ± 3.4	-11.7 ± 4.1	-5.6 ± 3.6	-14.8 ± 4.2	-4.3 ± 3.3	1.9 ± 4.1
p	-29.5 ± 4.8	-29.3 ± 4.5	-25.9 ± 4.1	-54.7 ± 4.5	-33.9 ± 5.4	-34.9 ± 5.0
1st Barrel Superlayer $\|z\|<345$cm						
n	-3.3 ± 4.4	-17.0 ± 3.6	-11.8 ± 3.5	-5.0 ± 3.3	-3.0 ± 3.6	4.4 ± 3.8
γ	-7.4 ± 6.4	-6.0 ± 8.8	-15.2 ± 5.7	-12.4 ± 6.2	2.3 ± 9.2	5.5 ± 6.4
μ	0.0 ± 0.0	0.0 ± 0.0	0.0 ± 0.0	0.0 ± 0.0	0.0 ± 0.0	0.0 ± 0.0
$h^{\pm}$	0.0 ± 0.0	0.0 ± 0.0	0.0 ± 0.0	0.0 ± 0.0	0.0 ± 0.0	0.0 ± 0.0
$e^{\pm}$	-83.2 ± 29.3	14.8 ± 46.0	38.7 ± 75.2	-39.2 ± 35.6	88.4 ± 138.4	14.2 ± 48.9
$\pi^{\pm}$	0.0 ± 0.0	0.0 ± 0.0	0.0 ± 0.0	0.0 ± 0.0	0.0 ± 0.0	0.0 ± 0.0
p	0.0 ± 0.0	0.0 ± 0.0	0.0 ± 0.0	0.0 ± 0.0	0.0 ± 0.0	0.0 ± 0.0
1st Barrel Superlayer end						
n	-4.2 ± 5.6	-24.0 ± 5.2	-17.7 ± 4.9	-3.8 ± 6.1	-3.0 ± 5.5	-0.3 ± 4.7
γ	-3.2 ± 7.5	-9.1 ± 6.9	2.1 ± 17.1	-2.7 ± 5.4	-1.1 ± 7.1	2.1 ± 6.7
μ	0.0 ± 0.0	0.0 ± 0.0	0.0 ± 0.0	0.0 ± 0.0	0.0 ± 0.0	0.0 ± 0.0
$h^{\pm}$	0.0 ± 0.0	0.0 ± 0.0	0.0 ± 0.0	0.0 ± 0.0	0.0 ± 0.0	0.0 ± 0.0
$e^{\pm}$	26.8 ± 32.8	11.4 ± 33.1	-22.1 ± 29.4	10.1 ± 28.8	49.7 ± 40.4	2.0 ± 35.7
$\pi^{\pm}$	0.0 ± 0.0	0.0 ± 0.0	0.0 ± 0.0	0.0 ± 0.0	0.0 ± 0.0	0.0 ± 0.0
p	0.0 ± 0.0	0.0 ± 0.0	0.0 ± 0.0	0.0 ± 0.0	0.0 ± 0.0	0.0 ± 0.0
2nd Barrel Superlayer $\|z\|<740$cm						
n	-1.2 ± 3.3	-17.5 ± 3.2	-15.0 ± 2.9	-1.6 ± 3.0	2.5 ± 3.1	7.3 ± 2.7
γ	1.6 ± 5.5	-14.1 ± 4.0	-9.9 ± 4.6	2.6 ± 5.9	11.0 ± 5.3	60.7 ± 44.5
μ	0.0 ± 0.0	0.0 ± 0.0	0.0 ± 0.0	0.0 ± 0.0	0.0 ± 0.0	0.0 ± 0.0
$h^{\pm}$	0.0 ± 0.0	0.0 ± 0.0	0.0 ± 0.0	0.0 ± 0.0	0.0 ± 0.0	0.0 ± 0.0
$e^{\pm}$	-18.0 ± 31.8	-11.5 ± 32.7	-46.3 ± 23.0	65.6 ± 87.0	-16.4 ± 26.4	-24.2 ± 28.5
$\pi^{\pm}$	0.0 ± 0.0	0.0 ± 0.0	0.0 ± 0.0	0.0 ± 0.0	0.0 ± 0.0	0.0 ± 0.0
p	0.0 ± 0.0	0.0 ± 0.0	0.0 ± 0.0	0.0 ± 0.0	0.0 ± 0.0	0.0 ± 0.0

Percentage change with respect to AV5

	AV5 11	AV5 41	AV5 5	AV5 6	AV5 7	AV5 71
2nd Barrel Superlayer end						
n	0.0 ± 3.8	-17.5 ± 2.9	-15.9 ± 3.0	-0.6 ± 4.8	1.3 ± 3.6	7.4 ± 3.2
γ	9.9 ± 7.0	-2.9 ± 8.6	-12.8 ± 4.3	22.3 ± 20.1	-2.5 ± 4.5	9.9 ± 4.4
μ	0.0 ± 0.0	0.0 ± 0.0	0.0 ± 0.0	0.0 ± 0.0	0.0 ± 0.0	0.0 ± 0.0
$h^{\pm}$	0.0 ± 0.0	0.0 ± 0.0	0.0 ± 0.0	0.0 ± 0.0	0.0 ± 0.0	0.0 ± 0.0
$e^{\pm}$	21.1 ± 58.9	-7.9 ± 47.7	76.0 ± 114.0	-10.1 ± 50.4	26.9 ± 56.9	374.3 ± 203.0
$\pi^{\pm}$	0.0 ± 0.0	0.0 ± 0.0	0.0 ± 0.0	0.0 ± 0.0	0.0 ± 0.0	0.0 ± 0.0
p	0.0 ± 0.0	0.0 ± 0.0	0.0 ± 0.0	0.0 ± 0.0	0.0 ± 0.0	0.0 ± 0.0
3rd Barrel Superlayer $\|z\|<740$cm						
n	-1.0 ± 3.4	-16.8 ± 3.1	-16.0 ± 3.1	-2.0 ± 3.4	2.6 ± 3.3	6.5 ± 2.8
γ	-18.8 ± 18.4	-25.6 ± 18.3	-29.5 ± 18.1	-12.6 ± 19.1	-15.9 ± 18.0	25.1 ± 40.3
μ	0.0 ± 0.0	0.0 ± 0.0	0.0 ± 0.0	0.0 ± 0.0	0.0 ± 0.0	0.0 ± 0.0
$h^{\pm}$	0.0 ± 0.0	0.0 ± 0.0	0.0 ± 0.0	0.0 ± 0.0	0.0 ± 0.0	0.0 ± 0.0
$e^{\pm}$	-0.3 ± 18.5	-27.9 ± 17.2	-30.5 ± 15.2	-19.6 ± 18.9	1.3 ± 18.7	1.3 ± 16.5
$\pi^{\pm}$	0.0 ± 0.0	0.0 ± 0.0	0.0 ± 0.0	0.0 ± 0.0	0.0 ± 0.0	0.0 ± 0.0
p	0.0 ± 0.0	0.0 ± 0.0	0.0 ± 0.0	0.0 ± 0.0	0.0 ± 0.0	0.0 ± 0.0
3rd Barrel Superlayer end						
n	0.8 ± 3.9	-18.0 ± 3.3	-15.3 ± 3.7	-1.0 ± 3.3	6.5 ± 5.9	7.8 ± 3.1
γ	0.5 ± 4.5	-10.9 ± 5.9	-8.2 ± 7.7	-1.1 ± 4.2	0.0 ± 4.5	12.6 ± 5.9
μ	0.0 ± 0.0	0.0 ± 0.0	0.0 ± 0.0	0.0 ± 0.0	0.0 ± 0.0	0.0 ± 0.0
$h^{\pm}$	0.0 ± 0.0	0.0 ± 0.0	0.0 ± 0.0	0.0 ± 0.0	0.0 ± 0.0	0.0 ± 0.0
$e^{\pm}$	5.4 ± 18.0	-17.4 ± 17.0	-16.1 ± 18.3	12.3 ± 30.4	30.4 ± 23.5	1.9 ± 21.9
$\pi^{\pm}$	0.0 ± 0.0	0.0 ± 0.0	0.0 ± 0.0	0.0 ± 0.0	0.0 ± 0.0	0.0 ± 0.0
p	0.0 ± 0.0	0.0 ± 0.0	0.0 ± 0.0	0.0 ± 0.0	0.0 ± 0.0	0.0 ± 0.0
1st Forward Superlayer $\eta<1.44$						
n	2.5 ± 4.0	-23.6 ± 3.6	-20.4 ± 3.4	1.3 ± 3.7	0.6 ± 4.0	13.4 ± 6.3
γ	3.8 ± 6.0	-16.0 ± 6.2	-10.9 ± 5.5	-0.9 ± 6.3	0.0 ± 5.7	15.4 ± 6.1
μ	0.0 ± 0.0	0.0 ± 0.0	0.0 ± 0.0	0.0 ± 0.0	0.0 ± 0.0	0.0 ± 0.0
$h^{\pm}$	0.0 ± 0.0	0.0 ± 0.0	0.0 ± 0.0	0.0 ± 0.0	0.0 ± 0.0	0.0 ± 0.0
$e^{\pm}$	3.4 ± 34.6	-58.5 ± 30.7	134.5 ± 169.8	-23.7 ± 33.4	-16.1 ± 34.4	-40.8 ± 31.6
$\pi^{\pm}$	0.0 ± 0.0	0.0 ± 0.0	0.0 ± 0.0	0.0 ± 0.0	0.0 ± 0.0	0.0 ± 0.0
p	0.0 ± 0.0	0.0 ± 0.0	0.0 ± 0.0	0.0 ± 0.0	0.0 ± 0.0	0.0 ± 0.0
1st Forward Superlayer $2.0>\eta>1.44$						
n	-2.2 ± 3.6	-25.5 ± 2.8	-24.7 ± 3.1	-1.8 ± 3.6	-0.6 ± 3.7	3.8 ± 3.2
γ	-3.5 ± 5.3	-25.6 ± 4.2	-22.2 ± 4.1	-4.6 ± 6.2	-1.2 ± 5.3	12.0 ± 6.7
μ	0.0 ± 0.0	0.0 ± 0.0	0.0 ± 0.0	0.0 ± 0.0	0.0 ± 0.0	0.0 ± 0.0
$h^{\pm}$	0.0 ± 0.0	0.0 ± 0.0	0.0 ± 0.0	0.0 ± 0.0	0.0 ± 0.0	0.0 ± 0.0
$e^{\pm}$	-18.8 ± 19.9	-18.9 ± 20.8	-5.8 ± 23.3	-13.8 ± 18.2	20.9 ± 26.3	-18.2 ± 20.7
$\pi^{\pm}$	0.0 ± 0.0	0.0 ± 0.0	0.0 ± 0.0	0.0 ± 0.0	0.0 ± 0.0	0.0 ± 0.0
p	0.0 ± 0.0	0.0 ± 0.0	0.0 ± 0.0	0.0 ± 0.0	0.0 ± 0.0	0.0 ± 0.0
1st Forward Superlayer $2.7>\eta>2.0$						
n	-1.3 ± 4.4	-24.2 ± 3.0	-22.8 ± 3.3	-1.3 ± 3.9	1.3 ± 3.7	6.0 ± 3.2
γ	-17.9 ± 7.0	-27.9 ± 7.6	-32.9 ± 7.2	-13.6 ± 7.1	-16.4 ± 7.1	-8.6 ± 7.0
μ	0.0 ± 0.0	0.0 ± 0.0	0.0 ± 0.0	0.0 ± 0.0	0.0 ± 0.0	0.0 ± 0.0
$h^{\pm}$	0.0 ± 0.0	0.0 ± 0.0	0.0 ± 0.0	0.0 ± 0.0	0.0 ± 0.0	0.0 ± 0.0
$e^{\pm}$	-33.1 ± 31.5	-57.8 ± 25.7	-15.9 ± 33.0	7.1 ± 33.6	-25.7 ± 29.9	50.0 ± 65.3
$\pi^{\pm}$	0.0 ± 0.0	0.0 ± 0.0	0.0 ± 0.0	0.0 ± 0.0	0.0 ± 0.0	0.0 ± 0.0
p	0.0 ± 0.0	0.0 ± 0.0	0.0 ± 0.0	0.0 ± 0.0	0.0 ± 0.0	0.0 ± 0.0

Percentage change with respect to AV5

	AV5 11	AV5 41	AV5 5	AV5 6	AV5 7	AV5 71
2nd Forward Superlayer η<1.44						
n	-0.4 ± 3.5	-17.2 ± 3.5	-18.3 ± 2.9	-2.0 ± 3.2	0.7 ± 3.4	9.2 ± 3.2
γ	-0.5 ± 4.6	-19.0 ± 4.1	-4.2 ± 14.1	-1.1 ± 5.5	1.6 ± 6.8	14.3 ± 7.1
μ	0.0 ± 0.0	0.0 ± 0.0	0.0 ± 0.0	0.0 ± 0.0	0.0 ± 0.0	0.0 ± 0.0
$h^{\pm}$	0.0 ± 0.0	0.0 ± 0.0	0.0 ± 0.0	0.0 ± 0.0	0.0 ± 0.0	0.0 ± 0.0
$e^{\pm}$	2.6 ± 28.1	-28.3 ± 18.1	-17.2 ± 20.0	132.2 ± 113.5	5.2 ± 25.8	7.0 ± 22.9
$\pi^{\pm}$	0.0 ± 0.0	0.0 ± 0.0	0.0 ± 0.0	0.0 ± 0.0	0.0 ± 0.0	0.0 ± 0.0
p	0.0 ± 0.0	0.0 ± 0.0	0.0 ± 0.0	0.0 ± 0.0	0.0 ± 0.0	0.0 ± 0.0
2nd Forward Superlayer 2.0>η>1.44						
n	0.9 ± 4.2	-17.0 ± 3.7	-21.4 ± 3.1	1.0 ± 3.7	0.0 ± 3.9	4.3 ± 3.1
γ	6.4 ± 6.4	-11.6 ± 5.4	-15.3 ± 5.5	5.2 ± 7.3	5.6 ± 7.7	11.2 ± 5.1
μ	0.0 ± 0.0	0.0 ± 0.0	0.0 ± 0.0	0.0 ± 0.0	0.0 ± 0.0	0.0 ± 0.0
$h^{\pm}$	0.0 ± 0.0	0.0 ± 0.0	0.0 ± 0.0	0.0 ± 0.0	0.0 ± 0.0	0.0 ± 0.0
$e^{\pm}$	6.5 ± 17.6	-25.8 ± 15.1	-16.7 ± 15.4	14.0 ± 17.8	39.2 ± 28.2	-4.8 ± 18.3
$\pi^{\pm}$	0.0 ± 0.0	0.0 ± 0.0	0.0 ± 0.0	0.0 ± 0.0	0.0 ± 0.0	0.0 ± 0.0
p	0.0 ± 0.0	0.0 ± 0.0	0.0 ± 0.0	0.0 ± 0.0	0.0 ± 0.0	0.0 ± 0.0
2nd Forward Superlayer 2.7>η>2.0						
n	10.8 ± 6.1	-5.4 ± 4.4	-10.0 ± 4.8	0.9 ± 4.1	6.3 ± 5.1	6.3 ± 4.5
γ	-6.6 ± 19.5	-34.8 ± 18.3	-32.1 ± 18.5	-3.6 ± 22.4	-22.5 ± 18.4	4.7 ± 25.3
μ	0.0 ± 0.0	0.0 ± 0.0	0.0 ± 0.0	0.0 ± 0.0	0.0 ± 0.0	0.0 ± 0.0
$h^{\pm}$	0.0 ± 0.0	0.0 ± 0.0	0.0 ± 0.0	0.0 ± 0.0	0.0 ± 0.0	0.0 ± 0.0
$e^{\pm}$	42.3 ± 41.4	0.3 ± 43.4	42.9 ± 43.6	7.1 ± 38.8	-3.5 ± 37.5	26.8 ± 40.6
$\pi^{\pm}$	0.0 ± 0.0	0.0 ± 0.0	0.0 ± 0.0	0.0 ± 0.0	0.0 ± 0.0	0.0 ± 0.0
p	0.0 ± 0.0	0.0 ± 0.0	0.0 ± 0.0	0.0 ± 0.0	0.0 ± 0.0	0.0 ± 0.0
3rd Forward Superlayer r>600						
n	1.0 ± 3.5	-16.8 ± 3.1	-16.5 ± 2.5	3.4 ± 4.3	-1.3 ± 3.6	6.7 ± 2.8
γ	-3.6 ± 4.7	-17.9 ± 4.1	-13.5 ± 5.1	4.5 ± 4.1	0.0 ± 4.7	21.8 ± 8.6
μ	0.0 ± 0.0	0.0 ± 0.0	0.0 ± 0.0	0.0 ± 0.0	0.0 ± 0.0	0.0 ± 0.0
$h^{\pm}$	0.0 ± 0.0	0.0 ± 0.0	0.0 ± 0.0	0.0 ± 0.0	0.0 ± 0.0	0.0 ± 0.0
$e^{\pm}$	-26.8 ± 13.6	-9.4 ± 17.3	-20.6 ± 14.8	-9.6 ± 15.3	1.5 ± 16.3	-1.9 ± 14.1
$\pi^{\pm}$	0.0 ± 0.0	0.0 ± 0.0	0.0 ± 0.0	0.0 ± 0.0	0.0 ± 0.0	0.0 ± 0.0
p	0.0 ± 0.0	0.0 ± 0.0	0.0 ± 0.0	0.0 ± 0.0	0.0 ± 0.0	0.0 ± 0.0
3rd Forward Superlayer η<2.3 r<700(mid)						
n	-7.1 ± 3.9	-15.2 ± 4.9	-17.8 ± 4.3	0.7 ± 4.3	7.1 ± 6.3	3.4 ± 3.9
γ	-3.6 ± 7.6	-13.7 ± 8.3	-12.4 ± 7.2	8.0 ± 10.9	0.9 ± 7.5	12.5 ± 8.7
μ	0.0 ± 0.0	0.0 ± 0.0	0.0 ± 0.0	0.0 ± 0.0	0.0 ± 0.0	0.0 ± 0.0
$h^{\pm}$	0.0 ± 0.0	0.0 ± 0.0	0.0 ± 0.0	0.0 ± 0.0	0.0 ± 0.0	0.0 ± 0.0
$e^{\pm}$	-1.7 ± 20.7	-7.1 ± 24.1	37.5 ± 28.9	41.5 ± 35.2	24.2 ± 25.6	67.0 ± 35.8
$\pi^{\pm}$	0.0 ± 0.0	0.0 ± 0.0	0.0 ± 0.0	0.0 ± 0.0	0.0 ± 0.0	0.0 ± 0.0
p	0.0 ± 0.0	0.0 ± 0.0	0.0 ± 0.0	0.0 ± 0.0	0.0 ± 0.0	0.0 ± 0.0
3rd Forward Superlayer 2.7>η>2.3						
n	-5.0 ± 5.7	-16.3 ± 4.8	-21.6 ± 4.4	-1.7 ± 4.7	-7.0 ± 5.1	-0.7 ± 5.8
γ	-9.1 ± 7.4	-17.0 ± 6.9	-12.5 ± 9.0	1.9 ± 11.0	1.9 ± 8.6	1.9 ± 7.9
μ	0.0 ± 0.0	0.0 ± 0.0	0.0 ± 0.0	0.0 ± 0.0	0.0 ± 0.0	0.0 ± 0.0
$h^{\pm}$	0.0 ± 0.0	0.0 ± 0.0	0.0 ± 0.0	0.0 ± 0.0	0.0 ± 0.0	0.0 ± 0.0
$e^{\pm}$	93.1 ± 58.2	5.9 ± 46.1	48.5 ± 56.9	-17.4 ± 40.2	79.2 ± 51.8	27.7 ± 44.8
$\pi^{\pm}$	0.0 ± 0.0	0.0 ± 0.0	0.0 ± 0.0	0.0 ± 0.0	0.0 ± 0.0	0.0 ± 0.0
p	0.0 ± 0.0	0.0 ± 0.0	0.0 ± 0.0	0.0 ± 0.0	0.0 ± 0.0	0.0 ± 0.0

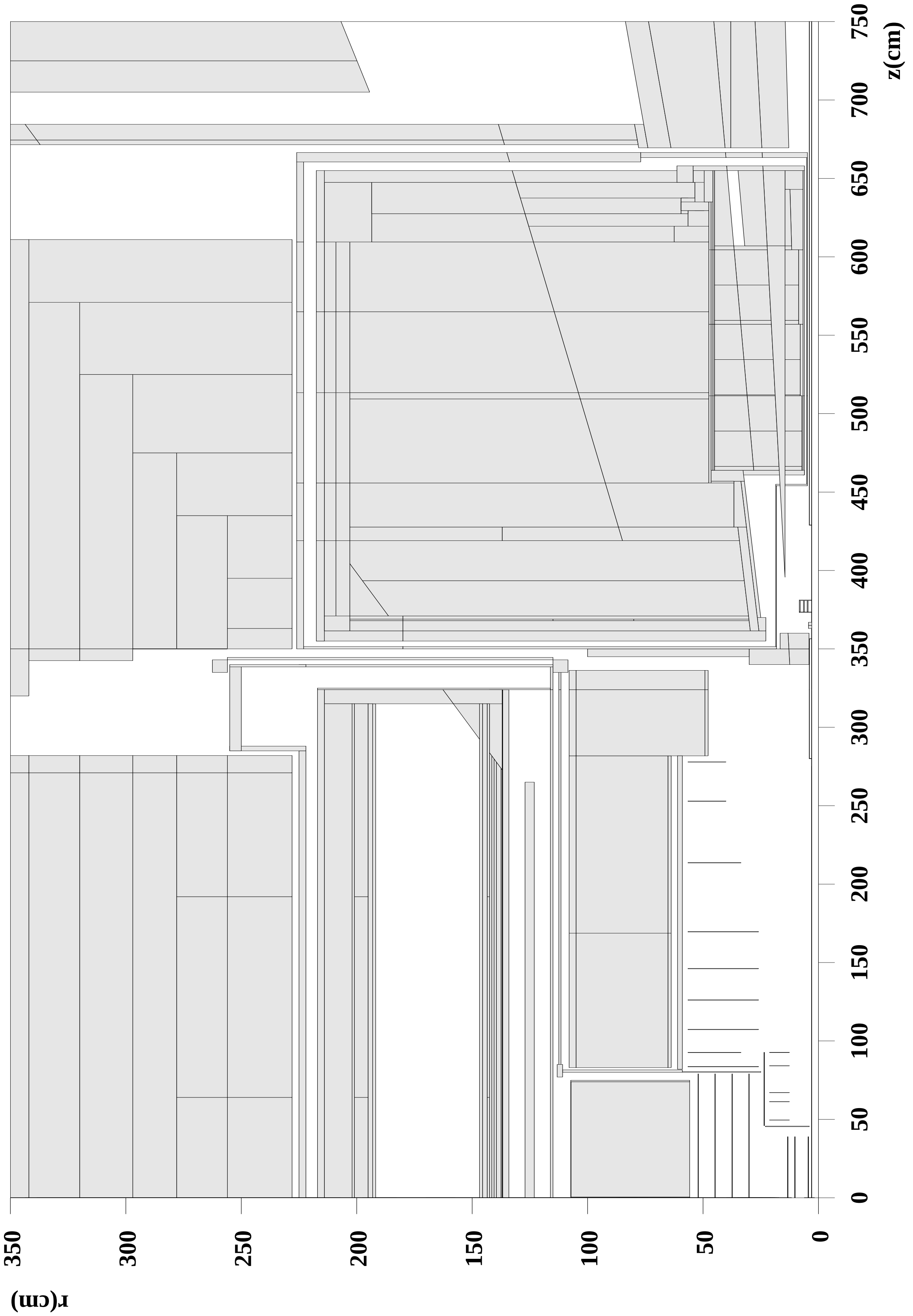

Figure 1: The AV5 baseline implementation of the inner part of the ATLAS Detector in FLUKA.

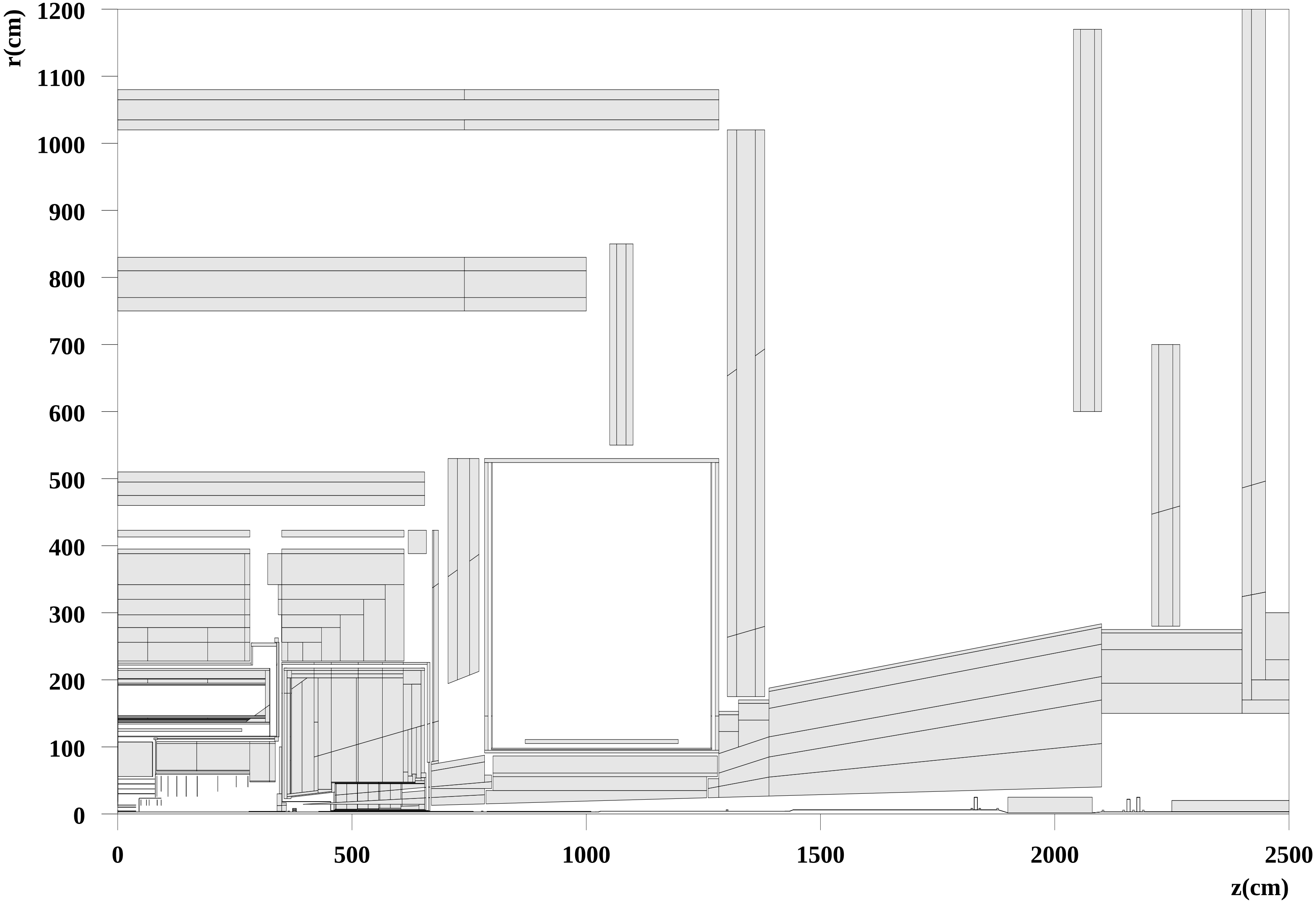

Figure 2: The AV5 baseline implementation of the ATLAS Detector in FLUKA.

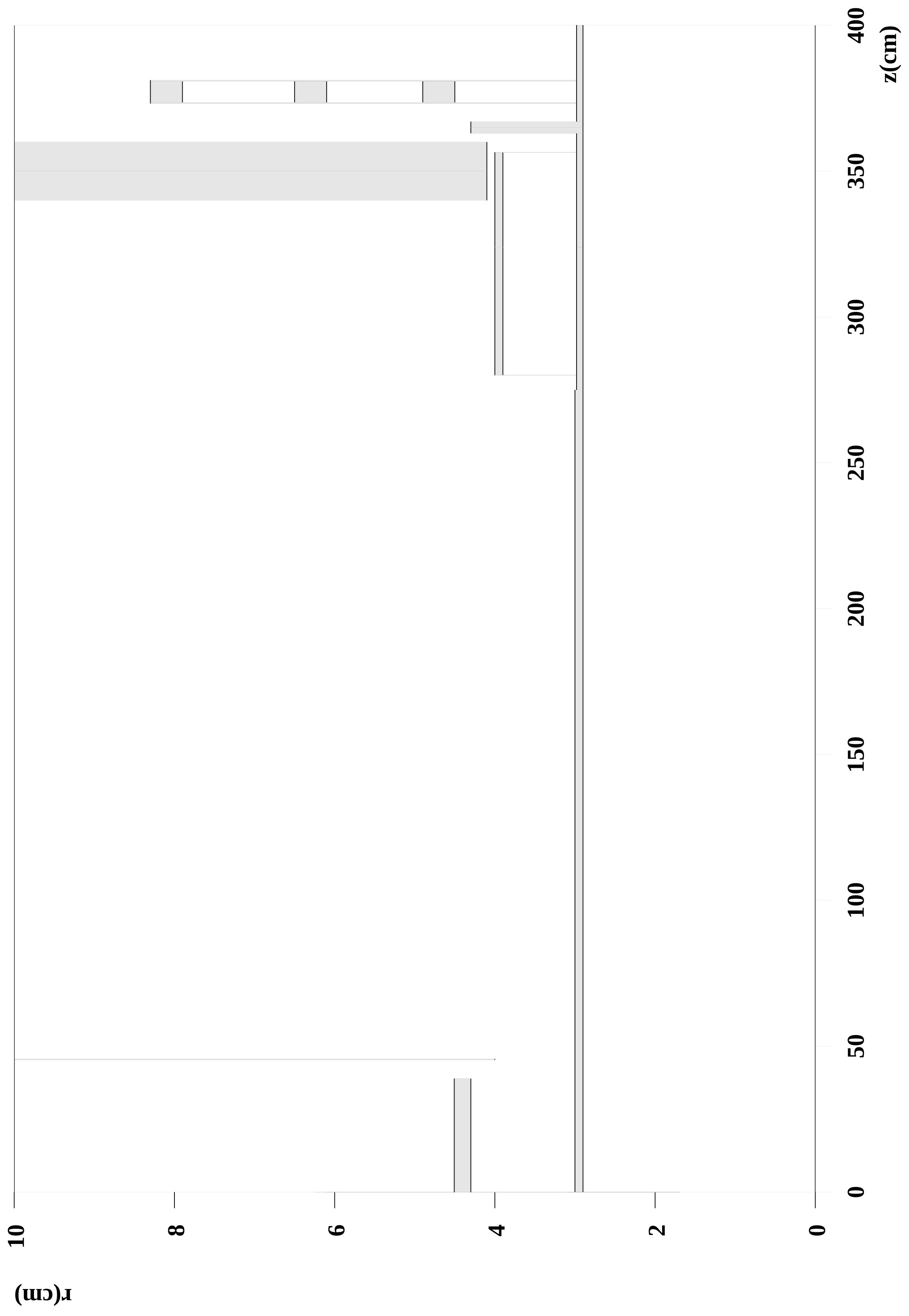

Figure 3: The AV5 baseline implementation of the VI section of the ATLAS beam pipe in FLUKA.

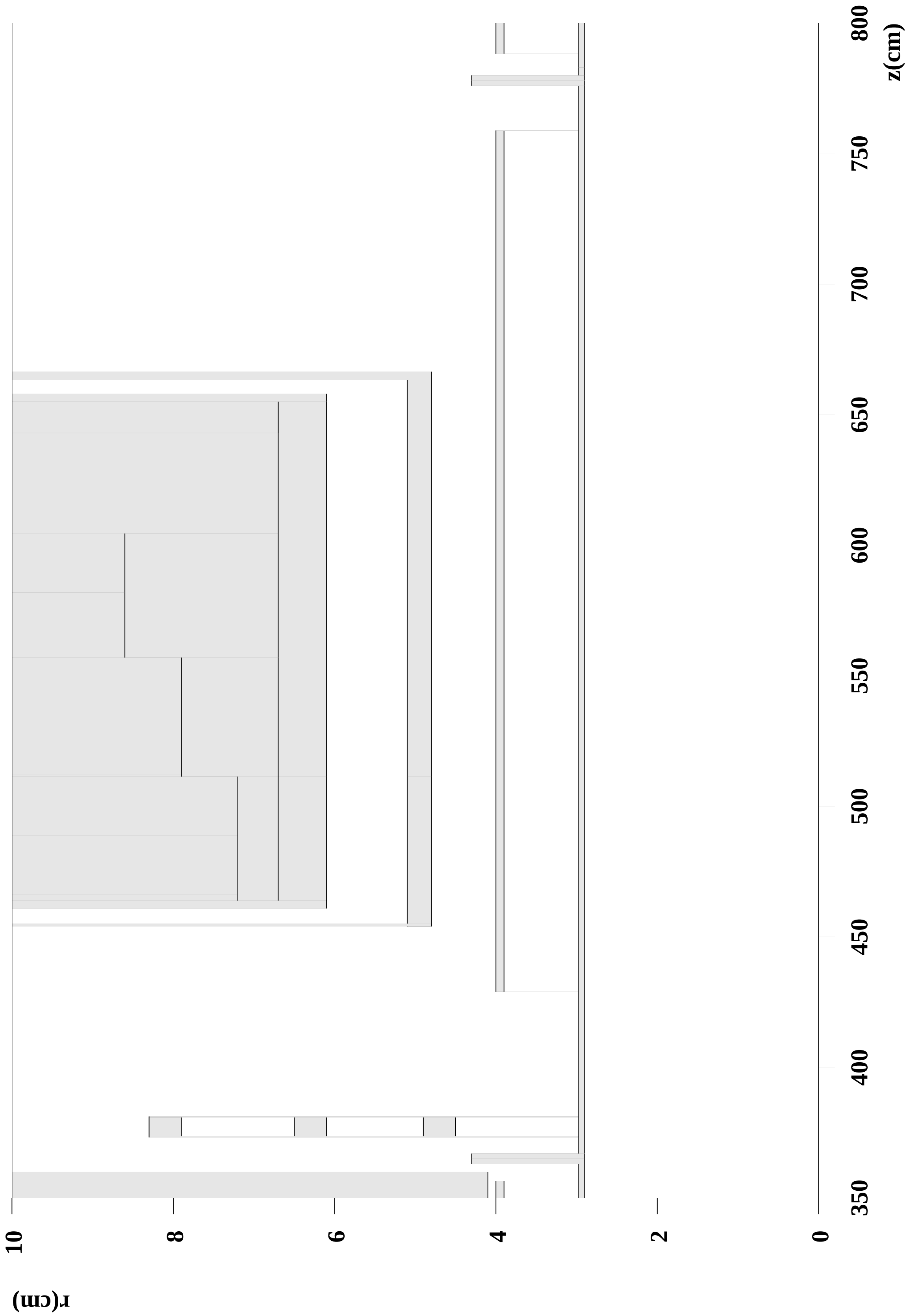

Figure 4: The AV5 baseline implementation of the VA section of the ATLAS beam pipe in FLUKA.

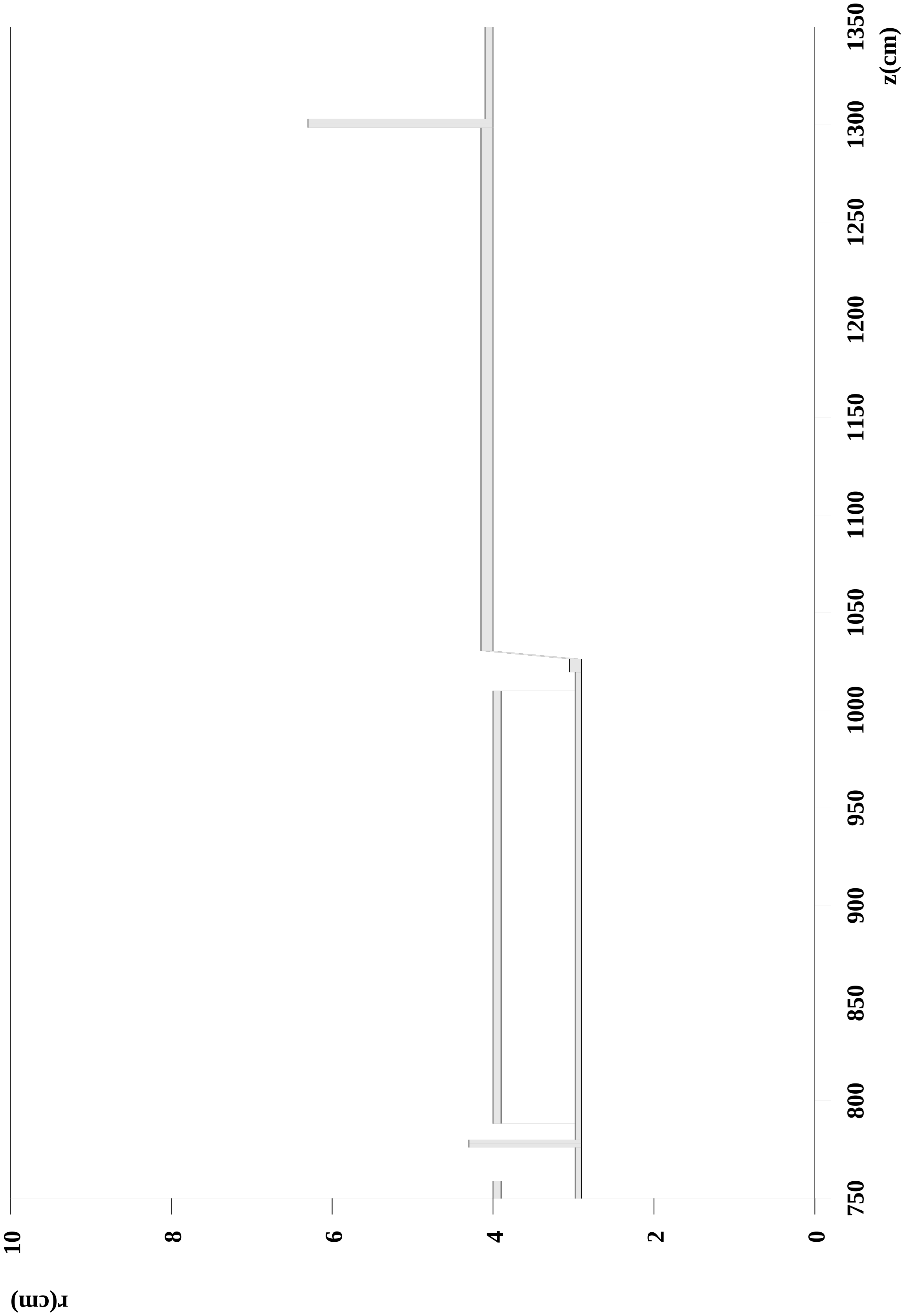

Figure 5: The AV5 baseline implementation of the VT section of the ATLAS beam pipe in FLUKA.

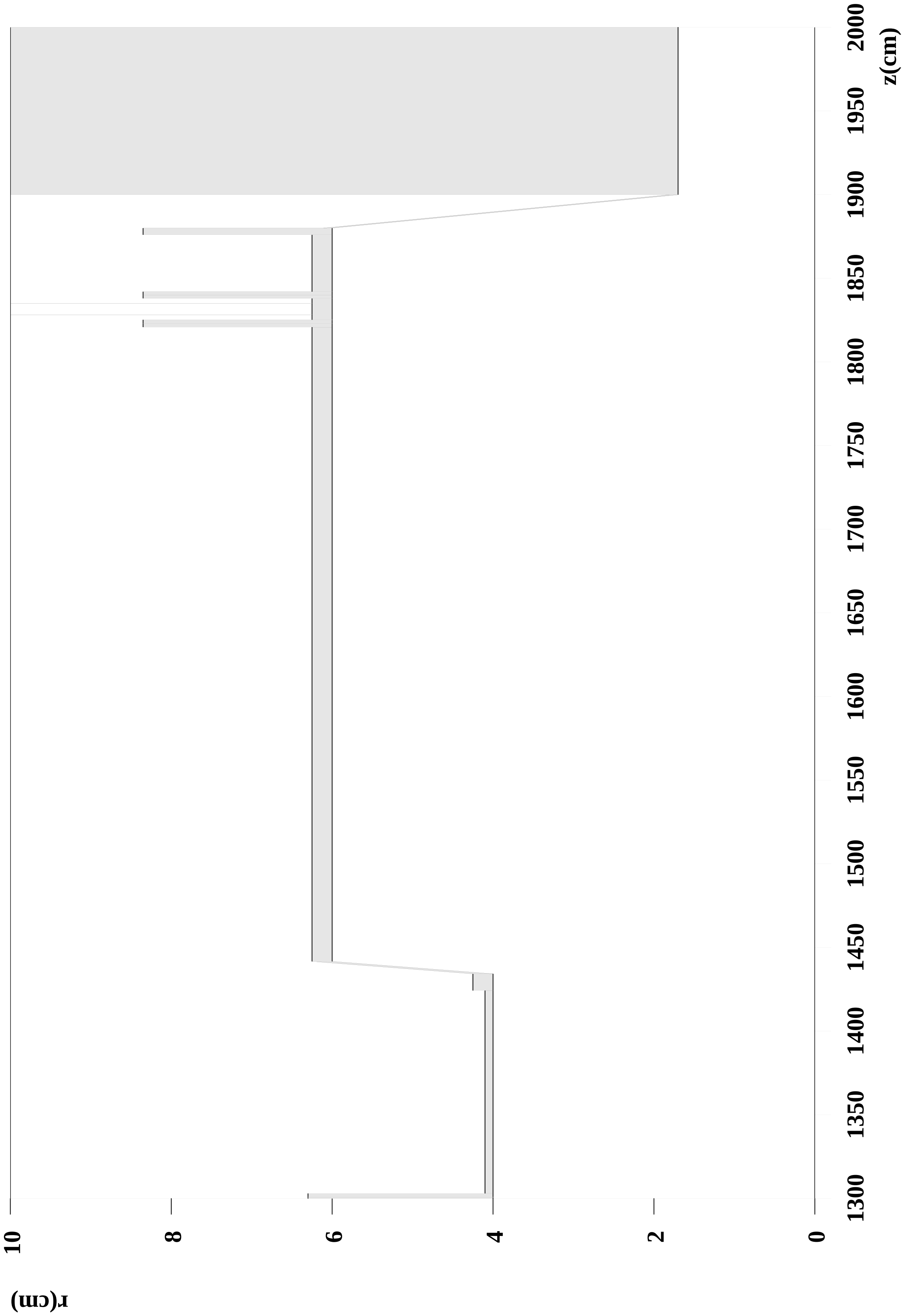

Figure 6: The AV5 baseline implementation of the VJ section of the ATLAS beam pipe in FLUKA.

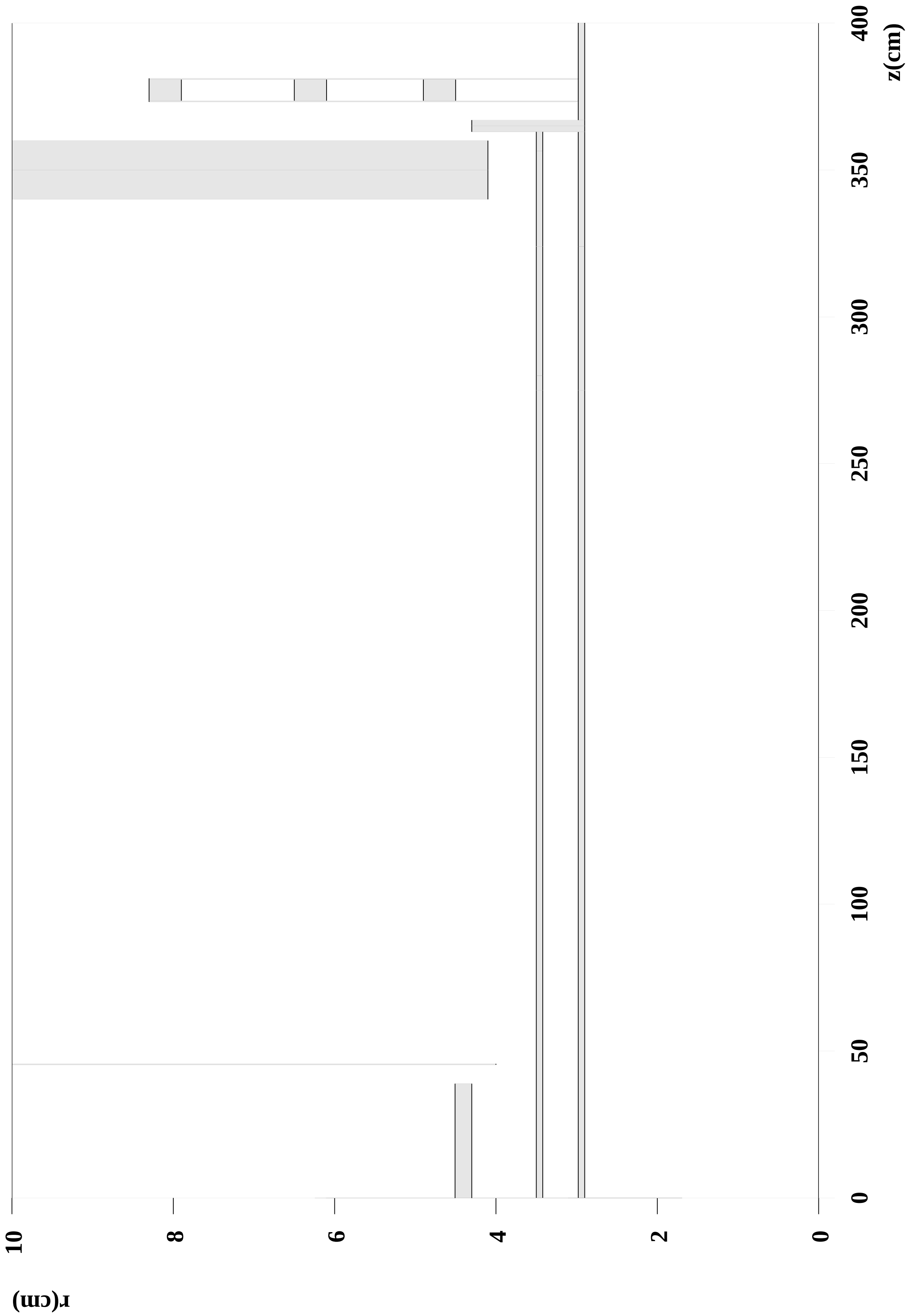

Figure 7: The AV5_6 implementation of the VI section of the ATLAS beam pipe in FLUKA.